ChemComm

Rhenium(V)-oxo corrolazines: isolating redox-active ligand reactivity

Journal:	*ChemComm*
Manuscript ID	CC-COM-09-2015-007956.R1
Article Type:	Communication
Date Submitted by the Author:	15-Oct-2015
Complete List of Authors:	Zaragoza, Jan Paulo; Johns Hopkins University, Department of Chemistry Siegler, Maxime; Johns Hopkins University, Chemistry Goldberg, David; Johns Hopkins University, Department of Chemistry

Journal Name

COMMUNICATION

Rhenium(V)-oxo corrolazines: isolating redox-active ligand reactivity†

Received 00th January 20xx,
Accepted 00th January 20xx

DOI: 10.1039/x0xx00000x

www.rsc.org/

Jan Paulo T. Zaragoza, Maxime A. Siegler, and David P. Goldberg*

The synthesis of the first example of a third-row metallocorrolazine characterized by single crystal X-ray diffraction is reported. This $Re^{V}(O)$ porphyrinoid complex shows an exclusively ligand-based reactivity with strong acids and oxidizing agents. The one-electron oxidized π-cation-radical complex is capable of H-atom abstraction.

The synthesis of rhenium complexes is of interest due to their potential use as catalysts for oxygen-transfer,[1] X–H (X = Si, B, P and H) bond activations,[2] and in CO_2 photoreduction reactions.[3] In addition, certain isotopes of rhenium are used in medical imaging, diagnostics, and therapeutics.[4] Although not found in natural heme systems, a few examples of rhenium porphyrins have been synthesized, including Buchler's first report of high-valent $Re^{V}(O)(X)$ porphyrins.[5] A decade later, the ring-contracted high-valent metal-oxo $Re^{V}(O)(TCF_3C)$ (TCF_3C = 5,10,15-tris(trifluoromethyl)corrole) was serendipitously prepared in an attempted porphyrin metallation reaction, providing the only example of a rhenium corrole.[6]

High-valent metal-oxo porphyrinoid complexes are of significant interest because of their role in synthetic and biological oxidation catalysis.[7] Our group recently described the characterization of high-valent $Mn^{V}(O)$ and $Cr^{V}(O)$ corrolazine (Cz) complexes by single crystal X-ray diffraction (XRD), and showed that these complexes exhibited dramatically different abilities to abstract hydrogen atoms from X–H (X = O, C) bonds.[8] In earlier efforts, it was also shown that the $Mn^{V}(O)(Cz)$ complex could be chemically oxidized to give $Mn^{V}(O)(Cz^{+\bullet})$, the first example of an $Mn^{V}(O)$ π-radical cation complex. The latter complex showed greatly enhanced O-atom transfer (OAT) reactivity compared to its neutral precursor.[9] Lewis/Brønsted acids (LA) were also shown to have a profound influence on $Mn^{V}(O)(Cz)$, stabilizing the valence tautomer $Mn^{IV}(O)(Cz^{+\bullet})(LA)$ and providing a rare example of a chemically driven, reversible valence tautomerization. The reactivity of $Mn^{IV}(O)(Cz^{+\bullet})(LA)$ was significantly different from $Mn^{V}(O)(Cz)$, with the metal-oxo unit and redox-active Cz ligand functioning together to carry out H-atom transfer (HAT) and OAT reactions.[10] Recently, much attention has been given to redox-active ligands and how they operate in conjunction with a metal ion to mediate various chemical transformations.[11]

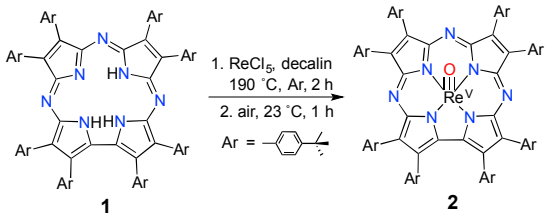

Scheme 1. Synthesis of $Re^{V}(O)(TBP_8Cz)$ (**2**).

Herein we report the synthesis and characterization by XRD of an $Re^{V}(O)(Cz)$ complex, the first metallocorrolazine containing a third-row metal ion, and a rare example of a structurally characterized rhenium porphyrinoid complex. This complex was prepared as an isoelectronic analog of $Mn^{V}(O)(Cz)$. Addition of strong Brønsted acids does not lead to stabilization of a valence tautomer in this case, but rather the reversible protonation of a remote site on the ligand. It is shown that the redox-active Cz ring can participate in electron-transfer and H-atom transfer reactions without the involvement of the metal-oxo unit. The H-atom transfer reactivity for the one-electron-oxidized $Re^{V}(O)(Cz^{+\bullet})$ is also shown to be strongly dependent on the nature of the external one-electron oxidant through a surprising observation of "zero-order" kinetics.

The synthesis of the $Re^{V}(O)$ corrolazine complex was accomplished by metallation of TBP_8CzH_3 (**1**) with excess $ReCl_5$ in refluxing decalin (Scheme 1). The product was purified by chromatography and gave $Re^{V}(O)(TBP_8Cz)$ (**2**) as a dark green solid (99% yield). The UV-vis spectrum of **2** exhibits a Soret band at 460 nm, which is the most red-shifted for any metallocorrolazine, and a Q-band at 670 nm. The ^1H NMR

Department of Chemistry, The Johns Hopkins University, 3400 N. Charles Street, Baltimore, MD 21218, USA
E-mail: dpg@jhu.edu

† Electronic Supplementary Information (ESI) available: Experimental, crystallographic, and computational details. CCDC 1426263 for **2**. For ESI and crystallographic data in CIF or other electronic format see DOI: 10.1039/x0xx00000x

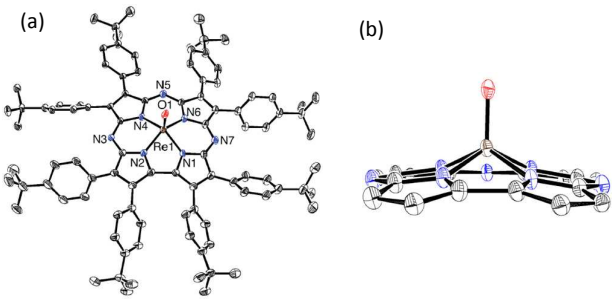

Fig. 1 Displacement ellipsoid plot (30% probability level) of $Re^{V}(O)(TBP_8Cz)$ (**2**). Selected bond distances (Å): Re–O, 1.682(5), Re–N_{ave}, 1.976, Re–N_{plane}, 0.739. a) Top view; b) side view (peripheral aryl groups were omitted). In both cases, the disorder and H-atoms were removed for clarity.

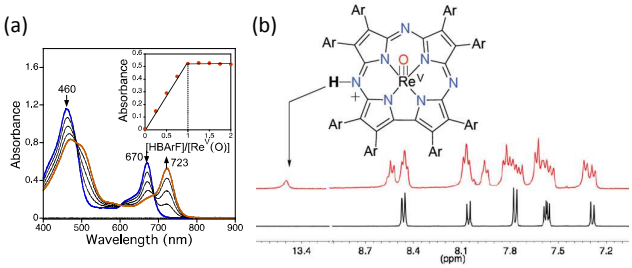

Fig. 2 a) UV-vis spectral changes upon addition of HBArF (0-2 equiv) to **2** in CH_2Cl_2. Inset: spectral titration at 723 nm showing maximal formation of product at 1 equiv HBArF. b) Comparison of ^{1}H NMR spectra (400 MHz) near the aryl region of **2** (black) and **3** (red) in CD_2Cl_2 at 23 °C.

spectrum of this complex is diamagnetic, consistent with a low-spin Re^{V} ion. Eight doublets appear between 8.44 – 7.26 ppm, which can be assigned to the peripheral *para*-substituted phenyl substituents (Fig. S1†). An LDI-TOF mass spectrum gives M^+ = 1557.38 *m/z*, in good agreement with the $Re(O)(TBP_8Cz)$ formulation.

Confirmation of the structure of **2** comes from single crystal X-ray crystallography. Single crystals of **2** were obtained by vapor diffusion of acetonitrile in toluene. The molecular structure is shown in Fig. 1, revealing a 5-coordinate Re center, with a terminal oxo ligand at a Re–O distance of 1.682(5) Å. This distance is consistent with an Re–O triple bond.[1e,12] The Re ion is displaced by *ca.* 0.74 Å from the plane defined by the four $N_{pyrrole}$ atoms. For comparison, $Re^{V}(O)(TCF_3C)$ exhibits an Re–O bond length of 1.662(2) Å and an out-of-plane distance of 0.701 Å.[6] The Re–O distance in **2** is significantly elongated compared to $Mn^{V}(O)$ (1.5455(18) Å) and $Cr^{V}(O)$ (1.553(2) Å) corrolazines,[8a] as expected for a third-row metal ion. The Re ion is also much further out of plane, by at least 0.2 Å, compared to either Mn^{V} or Cr^{V} complexes.

We previously found that $Mn^{V}(O)(TBP_8Cz)$ reacts with Lewis and Brønsted acids at 23 °C to give $Mn^{IV}(O)(TBP_8Cz^{\bullet+})(LA)$ (LA = H^+, Zn^{II}, $B(C_6F_5)_3$), in which the paramagnetic Mn^{IV} valence tautomer is stabilized over the diamagnetic, low-spin Mn^{V} species through a proposed weakening of the Mn–O π-bonding from coordination of LA to the terminal oxo group.[10] In contrast, the addition of the Brønsted acid $[H(OEt_2)_2][B(C_6F_5)_4]$ (HBArF) to $Mn^{V}(O)(TBP_8Cz)$ at low temperature (-60 °C) led to protonation of a remote *meso*-nitrogen atom on the Cz ring and retention of the low-spin Mn^{V} configuration. Protonation of the *meso*-N atoms in Mn^{III} corrolazines was also definitively confirmed by XRD.[13] To determine the reactivity of the isoelectronic $Re^{V}(O)$ analog toward Brønsted acids, the reaction of **2** with HBArF was examined. Addition of one equiv of HBArF to **2** in CH_2Cl_2 causes clear shifts in the UV-vis spectrum (Fig. 2a), although these changes are not consistent with formation of a Cz π-radical-cation. The final spectrum is more typical of protonation at the remote site on the Cz ligand.[13] Spectral titration with HBArF supports a 1:1 binding stoichiometry (inset, Fig. 2a) to form $[Re^{V}(O)(TBP_8Cz)(H)]^+$ (**3**).

Characterization of the monoprotonated complex **3** was performed by 1D (Fig. 2B) and 2D (Fig. S3-4†) NMR spectroscopy. The ^{1}H NMR spectrum of **3** is diamagnetic, confirming that the paramagnetic valence tautomer $Re^{IV}(O)(Cz^{+\bullet})$ is not observed. Spectra for **2** and **3** are shown in Fig. 2b (see Fig. S2†). A new peak is observed at 13.45 ppm for the protonated complex, and integrates to 1H. This peak can be assigned to protonation of a *meso*-N of the corrolazine ring, shifted downfield by the ring current effect. For comparison, the *meso* C–H proton of Zn octaethylporphyrin appears at *ca.* 10 ppm.[14] The aromatic pattern is complex, consistent with addition of H^+ to one of the *meso*-N atoms that does not lie on the mirror plane bisecting the pyrrole-pyrrole linkage. The NMR spectrum for **2** at 23 °C is similar to what was observed for protonation of $Mn^{V}(O)(TBP_8Cz)$ at -60 °C.[13]

The IR spectrum of **2** shows an intense peak at 997 cm^{-1} (Fig. 3a), in the region expected for the stretching frequency of an Re^{V}–O triple bond. However, an intense peak at ~997 cm^{-1} has also been observed in several other metallocorrolazines, and may arise from Cz vibrational modes.[15] To conclusively identify the Re–O stretch, we synthesized the isotopically labeled $Re^{V}(^{18}O)(TBP_8Cz)$ (**2-^{18}O**) by addition of excess $H_2{}^{18}O$ (80 equiv) to the Re metallation reaction involving TBP_8CzH_3 (**1**) and $ReCl_5$ in decalin. This method yielded the $Re^{V}(O)$ complex with >99% ^{18}O isotopic incorporation as seen by LDI-MS (Fig. S5†), and indicates a mechanism of oxygen incorporation that involves hydrolysis of an $Re^{V}(Cl)_2(TBP_8Cz)$ precursor.[5] The appearance of a new band upon ^{18}O substitution at 945 cm^{-1} is accompanied by a slight decrease in intensity of the band at 997 cm^{-1} (Fig. 3). These spectral changes are consistent with the $\nu(Re^{16}O)$ mode overlapping with the intense peak at 997 cm^{-1}. The predicted isotopic shift for ^{18}O substitution in an isolated Re–O diatomic oscillator is 52 cm^{-1}, in excellent agreement with the predicted value of $\nu(Re^{16}O)$ = 997 cm^{-1}. The Re-O stretch is close to that observed for $Re^{V}(O)$ corrole (994 cm^{-1}),[6] but higher than most $Re^{V}(O)$ porphyrins, phthalocyanines[5,12b] or N-confused porphyrin.[12a]

The effect of protonation on the Re–O bond can be probed by IR spectroscopy (Fig. 3b). Upon protonation of **2** with HBArF, a sharp peak at 3280 cm^{-1} appears, consistent with the N–H stretch of a *meso*-NH group (Fig. S6†). At the same time, the $\nu(Re^{18}O)$ peak at 945 cm^{-1} disappears, and only a broad band associated with $BArF^-$ is present at 975 cm^{-1} without any clear evidence for a new Re-^{18}O stretch. However, replacing HBArF with HOTf causes the broad peak at 975 cm^{-1} to disappear, revealing a new peak for $\nu(Re^{18}O)$ = 956 cm^{-1} (Fig. 3b). These data indicate that an 11 cm^{-1} blue shift occurs for

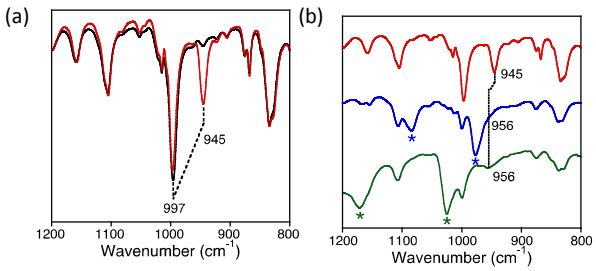

Fig. 3 ATR-IR spectra (800 – 1200 cm^{-1}) of a) **2**-^{16}O (black) and **2**-^{18}O (red), b) **2**-^{18}O (red), (**3**-^{18}O)(BArF$^-$) (blue), and (**3**-^{18}O)(OTf$^-$) (green). Asterisk (*) = peaks associated with OTf$^-$ or BArF$^-$ counterions.

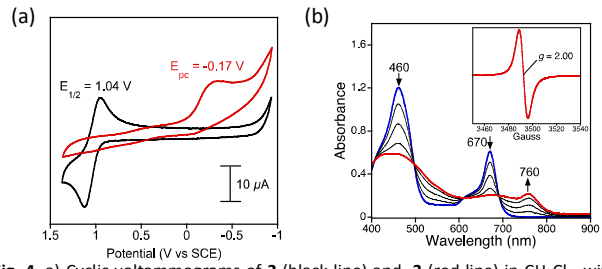

Fig. 4. a) Cyclic voltammograms of **2** (black line) and **3** (red line) in CH_2Cl_2, with 0.1 M $TBAPF_6$ supporting electrolyte, 150 mV/s. b) UV-vis spectral changes of **2** observed upon addition of $[Ar'_3N^{+\bullet}][SbCl_6^-]$ (0-1 equiv) in CH_2Cl_2. Inset: X-band EPR of $Re^V(O)(TBP_8Cz)^{+\bullet}$ (**4**) (3 mM) at 298 K in CH_2Cl_2.

the metal-oxo stretch, implicating a strengthening of the metal–oxo bond upon protonation of a remote site on the ligand.

Density functional theory (DFT) calculations were performed on complexes **2** and **3** to support structural and spectroscopic assignments. Geometry optimizations were performed at the PBE0/LANL2TZ/6-31G** level of theory, beginning with the crystal structure coordinates for **2**. The peripheral aryl substituents were replaced by H atoms to facilitate the calculations. The optimized geometry for **2** matched well with the experimentally determined crystal structure. Geometry optimizations for protonated **2** were performed with the H^+ attached at either the *meso*-N or the terminal oxo ligand. These calculations showed that the O–H tautomer is +29 kcal/mol higher in energy than the N–H tautomer **3** (Fig. S7†, Table S2†), and indicate that the *meso*-N is the preferred site of protonation. Frequency calculations give ν(Re–O) = 1055 cm^{-1} for **2** and 1064 cm^{-1} for **3**, which are both higher than the corresponding experimental values. DFT is known to overestimate vibrational frequencies due to systematic errors.[16] However, the difference between the calculated ν(Re–O) values for **2** and **3** ($\Delta\nu$(ReO) = 9 cm^{-1}) is in excellent agreement with experiment (11 cm^{-1}).

The $Mn^V(O)(TBP_8Cz)$ complex reacts rapidly with phosphine derivatives through an O-atom transfer mechanism.[10c] Attempts to react **2** with the phosphine derivatives PPh_3, PMe_3, or PEt_3 in CH_2Cl_2 at 23°C showed no reaction even over prolonged reaction times (5 d). Similarly, H-atom donors such as TEMPOH or 2,4-di-tert-butylphenol were unreactive toward **2**, although the isoelectronic $Mn^V(O)$ complex readily abstracts H-atoms from both of these substrates.[8b] Reduction of **2** with strong one-electron donors such as cobaltocene (E_{red} = -1.33 V vs SCE)[17] was also unsuccessful. We speculated that **3**, with an additional full unit of positive charge, might show enhanced oxidative reactivity compared to **2**, but reactions with PR_3 or ArOH substrates led only to deprotonation and recovery of **2.** Both the neutral and monoprotonated $Re^V(O)$ complexes appear inert to either H-atom or O-atom transfer reactions, suggesting a greatly enhanced stability for $Re^V(O)$ compared to $Mn^V(O)$ in the corrolazine environment.

To gain further insights into the reactivity of **2** and **3**, cyclic voltammetric measurements were performed (Fig. 4). Complex **2** exhibits a single reversible wave at 1.04 V vs SCE, which is close to an assigned Cz ring oxidation for $Mn^V(O)(TBP_8Cz)$,[9] as well as other metallocorrolazines.[15a] However, there are no other redox events observed for **2**, in contrast to the $Mn^V(O)$complex, which exhibits an Mn^V/Mn^{IV} couple near -0.05 V.[15] Upon protonation of **2**, the ring oxidation wave disappears, leaving only an irreversible reduction at -0.17 V as seen in the CV for **3**. Thus for **2** and **3** there are no clearly accessible metal-based redox couples, consistent with a lack of HAT and OAT reactivity. However, the reversible oxidation seen for **2** at 1.04 V suggested that a one-electron oxidized $Re^V(O)(Cz^{+\bullet})$ π-cation-radical complex might be accessible by chemical oxidation.[9,18]

Reaction of $Re^V(O)(TBP_8Cz)$ with $[Ar'_3N^{+\bullet}][SbCl_6^-]$ (Ar' = 4-BrC_6H_4, E_{red} = 1.16 V vs SCE)[17] resulted in isosbestic conversion to a new species with a broadened Soret peak at 445 nm and a relatively weak, red-shifted band at 760 nm (Figure 4b). These features are characteristic of a corrole,[19] porphyrazine,[20] and corrolazine π-radical.[9-10,18] Spectral titration showed one equiv of oxidant was required for complete formation of the π-radical cation complex (Fig. S8†). EPR spectroscopy revealed a sharp singlet at g = 2.00, similar to $Mn^V(O)$ and Mn^V(imido) Cz-π-radical cation species.[9,18] Quantitation of the EPR signal showed a 94% yield of the oxidized product. Attempts to isolate this product as a solid were unsuccessful, but taken together the data show that **2** can be oxidized in situ by $Ar'_3N^{+\bullet}$ to give the monocationic complex $Re^V(O)(TBP_8Cz^{+\bullet})$ (**4**).

In earlier work, dramatic enhancements in OAT reactivity were seen for $Mn^V(O)(TBP_8Cz^{+\bullet})$ compared to its neutral precursor,[9] but the Re^V analog **4** remained unreactive to OAT. Addition of phosphine derivatives to **4** in CH_2Cl_2 led only to 1-e^- reduction, restoring **2** with no evidence of oxo-transfer. However, addition of the H-atom donor 9,10-dihydroanthracene (DHA) to **4** resulted in quantitative conversion to monoprotonated **3**. Analysis by GC-FID showed anthracene was produced in 90% yield, confirming that formal HAT occurs via the net reaction in Scheme 2. Although these observations implied that **4** was abstracting an H-atom from DHA, UV-vis time course experiments under pseudo-first-order conditions (excess DHA) showed a surprising *linear*

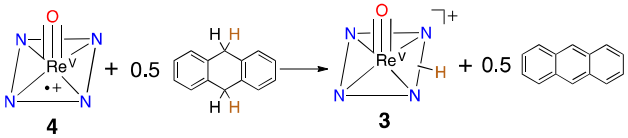

Scheme 2. Reaction of **4** with 9,10-DHA to form **3** and anthracene.

dependence for the decay of **4** and production of **3** (Fig. S10†). These data were indicative of a reaction *zero-order* in **4.** The zero-order kinetics can be explained by a mechanism involving back electron-transfer between Ar'_3N and **4**, establishing the equilibrium shown in Eq 1. The redox potentials for **2** and $[Ar'_3N^{+\bullet}][SbCl_6^-]$ indicate a relatively small K_{ET} = 107. The minor $Ar'_3N^{+\bullet}$ species can then oxidize DHA to give anthracene and Ar'_3N in the rate-determining step (Eq 2), while the released H^+ binds to **2** in preference to Ar'_3N (pKa ≤ -4).[21a] Independent experiments confirm that $[Ar'_3N^{+\bullet}][SbCl_6^-]$ oxidizes DHA to anthracene (98%) relatively rapidly in a second-order process (k = 0.126 M^{-1} s^{-1}) (Fig. S11†).

$$Re^{V}(O)(Cz) + Ar'_3N^{\bullet+} \rightleftharpoons Re^{V}(O)(Cz^{\bullet+}) + Ar'_3N \qquad (K_{ET}) \quad (1)$$

$$Ar'_3N^{\bullet+} + \mathbf{0.5}\ \text{DHA} \rightarrow Ar'_3N + \mathbf{0.5}\ \text{anthracene} + H^+ \qquad (k_1) \quad (2)$$

Replacement of $[Ar'_3N^{+\bullet}][SbCl_6^-]$ with the more powerful oxidant $Ce^{IV}(NH_4)_2(NO_3)_6$ (CAN, E_{red} = +1.33 V)[17] led to a distinct change in mechanism. Oxidation of **2** with CAN in CH_2Cl_2/CH_3CN (100:1 v/v) gives a UV-vis spectrum similar to **4**, and addition of excess DHA results in an *exponential decay* of **4** with the concomitant formation of **2** (Eq 3) (Fig. S12†). These data are consistent with a pseudo-first-order process. The use of the stronger oxidant CAN greatly disfavors back electron-transfer. In this case, the rate-determining step involves the direct reaction of **4** with DHA, and variation of [DHA] leads to a k_2 = 6.3 x 10^{-3} M^{-1} s^{-1}. This reaction likely occurs through an HAT mechanism between DHA and **4** to give **3**, which is then rapidly deprotonated by the NO_3^- counterion[21b] to give **2**. Control experiments show that **3** is rapidly deprotonated by $Bu_4N^+NO_3^-$ (Fig. S14†).

$$Re^{V}(O)(Cz^{\bullet+})(NO_3^-) \rightarrow Re^{V}(O)(Cz) + H^+NO_3^- \qquad (k_2) \quad (3)$$
$$+\ \mathbf{0.5}\ \text{DHA} \qquad\qquad +\ \mathbf{0.5}\ \text{anthracene}$$

We have reported the synthesis and XRD characterization of the first third-row metallocorrolazine. This $Re^{V}(O)$ complex is strikingly inert to both H-atom and O-atom transfer reactions, in contrast to its isoelectronic $Mn^{V}(O)$ analog. Protonation of **2** gives a cationic $Re^{V}(O)$ complex and no evidence of valence tautomerism, supporting the conclusion that protonation occurs exclusively on the *meso*-N atom and not on the oxo ligand. Taking advantage of the inertness of the Re–O group, we have provided the first insights into the reactivity of a porphyrinoid π-radical-cation completely decoupled from its high-valent metal-oxo core. This Cz π-radical-cation, which contains a weakly basic *meso*-N site, appears to be competent to abstract H-atoms from relatively weak C-H substrates. These observations suggest that porphyrin π-radical cations, including those found in heme enzyme metal-oxo intermediates, may have as yet unidentified roles to play in oxidative reactivity.

The authors acknowledge research support by the NIH (Grant GM101153 to D.P.G.). The Kirin cluster at JHU KSAS is thanked for CPU time to J.P.Z. We also thank J. Tang and A. Majumdar (JHU) for NMR assistance and T. Yang and A. Confer for helpful discussions.

Notes and references

1 (*a*) K. P. Gable and E. C. Brown, *J. Am. Chem. Soc.*, 2003, **125**, 11018-11026; (*b*) M. M. Abu-Omar, *Chem. Commun.*, 2003, 2102-2111; (*c*) J. L. Smeltz, C. P. Lilly, P. D. Boyle and E. A. Ison, *J. Am. Chem. Soc.*, 2013, **135**, 9433-9441; (*d*) S. Das and A. Chakravorty, *Eur. J. Inorg. Chem.*, 2006, **2006**, 2285-2291; (*e*) T. Yamamoto, M. Toganoh and H. Furuta, *Dalton Trans.*, 2012, **41**, 9154-9157.

2 (*a*) S. C. Sousa, I. Cabrita and A. C. Fernandes, *Chem. Soc. Rev.*, 2012, **41**, 5641-5653; (*b*) E. A. Ison, E. R. Trivedi, R. A. Corbin and M. M. Abu-Omar, *J. Am. Chem. Soc.*, 2005, **127**, 15374-15375.

3 (*a*) J. Hawecker, J.-M. Lehn and R. Ziessel, *J. Chem. Soc., Chem. Commun.*, 1983, 536-538; (*b*) C. D. Windle, M. V. Campian, A. K. Duhme-Klair, E. A. Gibson, R. N. Perutz and J. Schneider, *Chem. Commun.*, 2012, **48**, 8189-8191; (*c*) C. D. Windle, M. W. George, R. N. Perutz, P. A. Summers, X. Z. Sun and A. C. Whitwood, *Chem. Sci.*, 2015.

4 (*a*) E. John, M. L. Thakur, J. DeFulvio, M. R. McDevitt and I. Damjanov, *J. Nucl. Med.* , 1993, **34**, 260-267; (*b*) Z.-Y. Jia, H.-F. Deng, M.-F. Pu and S.-Z. Luo, *Eur. J. Nucl. Med. Mol. Imaging*, 2008, **35**, 734-742.

5 J. W. Buchler and S. B. Kruppa, *Z. Naturforsch. B*, 1990, **45**, 518-530.

6 M. Kin Tse, Z. Zhang and K. S. Chan, *Chem. Commun.*, 1998, 1199-1200.

7 (*a*) Z. Gross, *J. Biol. Inorg. Chem.*, 2001, **6**, 733-738; (*b*) H. M. Neu, R. A. Baglia and D. P. Goldberg, *Acc. Chem. Res.*, 2015, DOI: 10.1021/acs.accounts.5b00273; (*c*) M. Sono, M. P. Roach, E. D. Coulter and J. H. Dawson, *Chem. Rev.*, 1996, **96**, 2841-2888; (*d*) M. T. Green, *Curr. Opin. Chem. Biol.*, 2009, **13**, 84-88.

8 (*a*) R. A. Baglia, K. A. Prokop-Prigge, H. M. Neu, M. A. Siegler and D. P. Goldberg, *J. Am. Chem. Soc.*, 2015, **137**, 10874-10877; (*b*) D. E. Lansky and D. P. Goldberg, *Inorg. Chem.*, 2006, **45**, 5119-5125.

9 K. A. Prokop, H. M. Neu, S. P. de Visser and D. P. Goldberg, *J. Am. Chem. Soc.*, 2011, **133**, 15874-15877.

10 (*a*) P. Leeladee, R. A. Baglia, K. A. Prokop, R. Latifi, S. P. de Visser and D. P. Goldberg, *J. Am. Chem. Soc.*, 2012, **134**, 10397-10400; (*b*) R. A. Baglia, M. Dürr, I. Ivanović-Burmazović and D. P. Goldberg, *Inorg. Chem.*, 2014, **53**, 5893-5895; (*c*) J. P. T. Zaragoza, R. A. Baglia, M. A. Siegler and D. P. Goldberg, *J. Am. Chem. Soc.*, 2015, **137**, 6531-6540.

11 (*a*) O. R. Luca and R. H. Crabtree, *Chem. Soc. Rev.*, 2013, **42**, 1440-1459; (*b*) P. J. Chirik, *Inorg. Chem.*, 2011, **50**, 9737-9740.

12 (*a*) T. Yamamoto, M. Toganoh, S. Mori, H. Uno and H. Furuta, *Chem. Sci.*, 2012, **3**, 3241-3248; (*b*) M. Göldner, L. Galich, U. Cornelisse and H. Homborg, *Z. Anorg. Allg. Chem.*, 2000, **626**, 985-995.

13 H. M. Neu, J. Jung, R. A. Baglia, M. A. Siegler, K. Ohkubo, S. Fukuzumi and D. P. Goldberg, *J. Am. Chem. Soc.*, 2015, **137**, 4614-4617.

14 R. J. Abraham, B. Evans and K. M. Smith, *Tetrahedron*, 1978, **34**, 1213-1220.

15 (*a*) A. J. McGown, Y. M. Badiei, P. Leeladee, K. A. Prokop, S. DeBeer and D. P. Goldberg, in *The Handbook of Porphyrin Science*, eds. K. M. Kadish, K. M. Smith and R. Guilard, World Scientific, New Jersey, 2011, vol. 14, ch. 66, pp. 525-600; (*b*) D. E. Lansky, B. Mandimutsira, B. Ramdhanie, M. Clausén, J. Penner-Hahn, S. A. Zvyagin, J. Telser, J. Krzystek, R. Zhan, Z. Ou, K. M. Kadish, L. Zakharov, A. L. Rheingold and D. P. Goldberg, *Inorg. Chem.*, 2005, **44**, 4485-4498.

16 T. R. Cundari and P. D. Raby, *J. Phys. Chem. A.*, 1997, **101**, 5783-5788.

17 N. G. Connelly and W. E. Geiger, *Chem. Rev.*, 1996, **96**, 877-910.

18 D. E. Lansky, J. R. Kosack, A. A. Narducci Sarjeant and D. P. Goldberg, *Inorg. Chem.*, 2006, **45**, 8477-8479.

19 P. Schweyen, K. Brandhorst, R. Wicht, B. Wolfram and M. Bröring, *Angew. Chem. Int. Ed.*, 2015, **54**, 8213-8216.

20 T. Yoshida, W. Zhou, T. Furuyama, D. B. Leznoff and N. Kobayashi, *J. Am. Chem. Soc.*, 2015, **137**, 9258-9261.

21 (*a*) E. M. Arnett, R. P. Quirk and J. J. Burke, *J. Am. Chem. Soc.*, 1970, **92**, 1260-1266; (*b*) O.W. Kolling, *Trans. Kans. Acad. Sci.,* 1965, 68, 575-581.